# Acidity and Catalytic Activity of a Nafion-H/Silica Nanocomposite Catalyst Compared with a Silica-Supported Nafion Sample

Béla Török,*,[1] Imre Kiricsi,† Árpád Molnár,*,[1] and George A. Olah‡

*Department of Organic Chemistry, University of Szeged, Dóm tér 8, H-6720 Szeged, Hungary; †Department of Applied and Environmental Chemistry, University of Szeged, Rerrich tér 1, H-6720 Szeged, Hungary; and ‡Department of Chemistry and Loker Hydrocarbon Research Institute, University of Southern California, Los Angeles, California 90089-1661

The characterization of acid sites in the recently developed Nafion-H/silica nanocomposite catalyst was carried out through pyridine adsorption using the surface FT-IR technique. For comparison, an impregnated Nafion-H/SiO$_2$ catalyst was also studied. A large number of free surface SO$_3$H groups was detected on the surface of the Nafion-H/silica nanocomposite, in contrast to the impregnated catalyst. Pyridine adsorption demonstrates that Brønsted as well as Lewis acid sites are present on the surface of the samples. There was a large number of available Brønsted sites on the surface of the Nafion-H/silica nanocomposite catalyst. As well as pyridine adsorption, the surface reaction of cyclopropane also revealed that the nanocomposite catalyst has a high number of acid sites. The impregnated sample exhibits much lower activity. The effect of different types of acidity and of acid strength were studied by means of the Friedel–Crafts alkylation (adamantylation of toluene) and various rearrangements. In agreement with the results of surface studies, the nanocomposite specimen exhibits activity which is several orders of magnitude higher than that observed for the other Nafion samples studied. This outstanding activity is attributed to the large surface area and to the increased accessibility of surface-active sites to reactants in catalytic transformations. © 2000 Academic Press

## INTRODUCTION

The ever-growing demand for environmentally safe industrial processes requires the development and use of effective and safe catalysts. Many acid catalysts are hazardous and corrosive, such as HF, sulfuric acid, and nitric acid (1). A plethora of solid acids are, however, already available to take the place of these aggressive and dangerous materials in the laboratory practice and in industry. Molecular sieves, such as HY and ZSM-5 zeolites (2) and heteropoly acids (3) have already been introduced into the industrial production of chemicals. Another class of solid acids is the acidic form of ion-exchanged polymers, which exhibit a wide range of acid strength, thermal stability, etc. Two important classes of these polymers are polystyrene-based materials (Amberlyst, Dowex) (4) and perfluorinated resinsulfonic acid based ion-exchanged resins (Nafion) (5). A new family of siloxane-based polymers, Deloxane, has recently been developed by Degussa (6).

Due to their structural features, the perfluorinated ion-exchanged polymers, commercially available under the tradename Nafion, show high acidity and activity in acid-catalyzed reactions (7). Nafion is a cross-linked perfluorinated polymeric sulfonic acid (8–10). Since the perfluoroalkyl environment and especially the $\alpha$-CF$_2$ moiety have high electron-withdrawing character, the acidity of the sulfonic acid groups is very high. Nafion resins exhibit an acidic character comparable to that of 100% sulfuric acid and triflic acid in trifluoroacetic anhydride solution. The Hammett acidity constant for Nafion-H was estimated to be $\sim-12$, i.e., it is a solid superacid (7, 11). Due to its superacidic character, chemical resistance, thermal stability, and ease of regeneration, Nafion-H is a frequently used solid acid catalyst in organic transformations (7). Nafion-H can take the place of common liquid acids in numerous transformations. However, the use of Nafion NR50 beads, which have an extremely low surface area ($\sim0.02$ m$^2$ g$^{-1}$), generally requires the use of relatively large amounts of catalyst and longer reaction times. Furthermore, the acid sites of Nafion NR50 are not easily accessible and, consequently, the rate of the gas phase reaction is rather low. Harmer and co-workers recently reported a method for overcoming this problem (12). They developed new solid superacidic catalysts called Nafion-H silica nanocomposites. They are highly active and have a large surface area (150–500 m$^2$ g$^{-1}$) with small (<100 nm) Nafion particles entrapped in the porous silica framework (12). Compared to Nafion-H beads, nafion particles have very high specific activity in 1-butene isomerization (13), in Friedel–Crafts alkylation and acylation (12), and in the nitration of benzene (12). These observations were further confirmed in other transformations, namely, in the dimerization of $\alpha$-methylstyrene (14), in the benzylation of aromatics (15), and in the Fries rearrangement (16).

[1] Corresponding authors.

We report here pyridine adsorption acidity measurements, made by surface FT-IR spectroscopy, to determine the Brønsted and Lewis acidity of this new, very promising solid acid catalyst. Catalytic properties were also studied in the ring opening of cyclopropane, in Friedel–Crafts alkylation (adamantylation of toluene), and in the ortho-Claisen and Fries rearrangements. In addition, comparative studies with Nafion beads and a silica-supported Nafion sample, prepared by impregnation, were carried out to illustrate the clear advantages of the nanostructured Nafion-H catalyst.

## EXPERIMENTAL

### Materials and Catalysts

Tetraethylorthosilicate [$Si(OC_2H_5)_4$] and the silica catalyst support ($S_{BET} = 500$ m$^2$/g) were purchased from Aldrich; Nafion-H is a commercially available Dupont product. The active H-form was generated from the potassium salt after being treated with 25% nitric acid, washed with water, and dried (105°C, 24 h) (7b). Nafion-H perfluorinated ion-exchanged solution (5% concentration), 1-bromoadamantane, pyridine, and the solvents were purchased from Aldrich and cyclopropane from Merck. Literature procedures were applied to synthesize allyl phenyl ether (17) and phenyl acetate (18). They proved to be 99% pure by GC.

Ten percent Nafion-H on a silica (10% Nafion-H/SiO$_2$) catalyst was prepared by impregnation. Ten grams of silica support was suspended in a 2-propanol/1-propanol/water mixture containing the calculated amount of Nafion-H. The mixture was stirred at room temperature for 2 h, the solvents were removed by a rotary evaporator, and the resulting free-flowing material was dried under vacuum (100°C, 5 Torr, 24 h). Nafion-H/silica nanoncomposite material with 13% Nafion was prepared using tetraethylorthosilicate according to a procedure described in the literature (12).

### Characterization of the Catalysts

*In situ* Fourier transform infrared spectroscopy (FT-IR) (Mattson Genesis 1 spectrometer) was used to characterize the acid centers of the catalysts. Self-supported wafers, ~10 mg/cm$^2$ thick, prepared from the powdered materials were placed into an IR-cell connected to a vacuum system. The samples were outgassed at 200°C and their spectra recorded.

In pyridine adsorption–desorption studies, 1.33 kPa of pyridine was introduced into the optical cell at 25°C followed by the registration of the spectrum related to the adsorbed pyridine species. Adsorption equilibrium was reached after 5 min as revealed by the spectra observed after the samples were treated with pyridine. The cell was evacuated, and the temperature was raised at regular intervals. After each heat treatment the IR cell was evacuated and the spectrum recorded at room temperature.

### Methods of Catalytic Studies

As well as pyridine adsorption, the ring-opening reaction of cyclopropane was used to characterize surface acidity. The surface reaction of cyclopropane was investigated in the same IR cell used for pyridine adsorption. Cyclopropane (1.33 kPa) reacted over the outgassed self-supported wafer and the spectrum was recorded. The change in the absorbance of the band at 3080 cm$^{-1}$, due to the adsorbed cyclopropane species, was considered to be a measure of the transformation of the surface.

The adamantylation of toluene was studied by refluxing and stirring 0.212 g (0.001 mol) of 1-bromoadamantane and 0.2 g of catalyst in 5 ml of toluene.

The Claisen rearrangement was carried out by refluxing a continuously stirred mixture of 2.01 g (0.015 mol) of allyl phenyl ether, 0.05 g of 1,3,5-tri-*tert*-butylbenzene (internal standard), and the catalyst (10 mg of Nafion-H beads or an appropriate amount of the supported catalysts containing the same amount of Nafion resin) in benzene (10 ml).

The Fries rearrangement was performed by reacting a stirred mixture of 0.544 g (0.004 mol) of phenyl acetate and 0.2 g of catalyst in 5 ml of nitrobenzene at 220°C. In one experiment a mixture of 2 ml of phenol and 3 ml of nitrobenzene was used as the solvent.

In each of the above reactions, products that were withdrawn at intervals were analyzed (GC) to determine conversions and compositions of the products (Carlo Erba Fractovap 2350 equipment, thermal conductivity detector, OV-17 column, or HP 5890 GC, FID detector, 60-m DB-1 column). Products were identified by GC-MS (HP 5890 GC coupled with a HP 5970 mass selective detector, 60-m DB-1 column).

## RESULTS AND DISCUSSION

### Characterization of Surface Acidity

The results of a systematic study of pyridine adsorption and the skeletal isomerization of cyclopropane, used to determine the type, the relative amount, and the strength of the acid centers of the two catalyst samples, are presented here. Both these techniques give important information with respect to the acidity of the samples and enable the determination of the correlation between acidity and activity.

Figure 1 shows the results of pyridine adsorption for the 10% Nafion-H/SiO$_2$ sample. In the spectrum registered after evacuation at room temperature, i.e., after the removal of gaseous and physically adsorbed pyridine, three bands, considered to be characteristic of acid sites developed (19–21) (Fig. 1b): a small, broad band at 1545 cm$^{-1}$, a somewhat sharper band at 1490 cm$^{-1}$, and a sharp, more intense
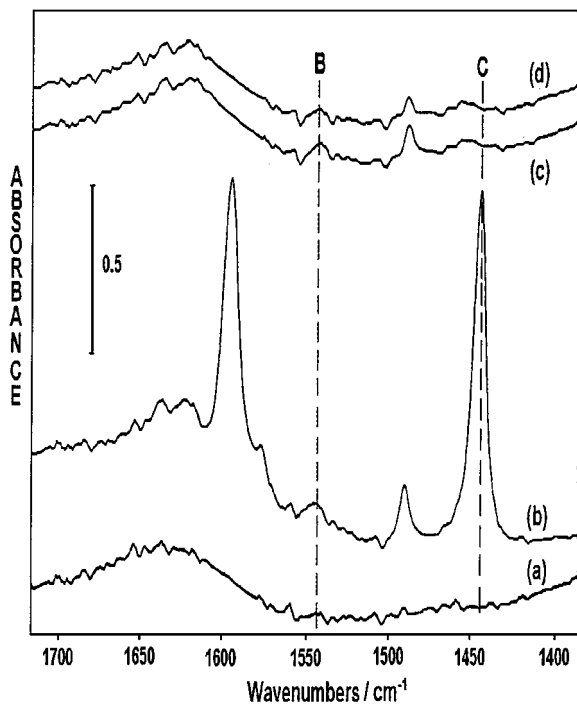
**FIG. 1.** FT-IR spectra illustrating pyridine adsorption on the 10% Nafion-H/SiO₂ sample. (B) Band characteristic of pyridine adsorbed on Brønsted sites. (C) Band characteristic of pyridine interacting with the silica matrix. (a) Without pyridine; after pyridine adsorption and evacuation at (b) room temperature, (c) 80°C, and (d) 150°C.

distinguish among different acid sites. Pyridine molecules bonded to Lewis acid sites (complexing pyridine) absorb at 1450 cm$^{-1}$ (ascribed to the 19b-ring mode of pyridine) while those adsorbed on Brønsted acid sites (pyridinium ion) show absorbance at 1540 cm$^{-1}$ as a result of the different types of surface bonding (19–21). The third band at 1490 cm$^{-1}$ is a combined band originating from pyridine that is bonded to both Brønsted and Lewis acid sites. The relative surface concentrations of Brønsted and Lewis acid sites can be determined by comparing the corresponding absorbance.

From the data presented in Figs. 1 and 2, it is obvious that both Brønsted and Lewis acid sites are present on the surface of the samples. The band at 1544–1545 cm$^{-1}$ is characteristic of the pyridinium ion resulting from the reaction of pyridine with proton sites. The band appearing at 1445–1450 cm$^{-1}$ represents the interaction of pyridine with the silica matrix through donor–acceptor-type bonds. It is also clear that this latter bonding is rather weak since complexed pyridine can be almost completely removed from the surface at 80°C. Pyridinium ions, in contrast, are more strongly bound to the surface. In the case of the nanocomposite sample, the intensity of the band changed only slightly, even at 150°C. Moreover, the nanocomposite material exhibits additional IR absorption at 1415 cm$^{-1}$. This band appeared in

band at 1445 cm$^{-1}$. After evacuation at 80°C, the band at 1445 cm$^{-1}$ disappeared (Fig. 1c), whereas the intensity of the band at 1540 cm$^{-1}$ decreased slightly. Further evacuation at 150°C resulted in a further decrease in the intensity of the latter band (Fig. 1d). The intensity of the band at 1490 cm$^{-1}$ decreased gradually.

The IR spectrum of the nanocomposite sample after evacuation showed a rather broad band at 1415 cm$^{-1}$ (Fig. 2a). Upon adsorption of pyridine, two characteristic changes were observed. As expected, all three bands associated with acid centers observed in the above experiments were detected (1544, 1490, and 1445 cm$^{-1}$) (Fig. 2b). At the same time, the band at 1415 cm$^{-1}$ disappeared. Upon evacuation at 80°C, the band at 1450 cm$^{-1}$ also disappeared (Fig. 2c). In sharp contrast, the band at 1544 cm$^{-1}$ remained almost unchanged. Evacuation at 150°C resulted in a slight decrease in the intensity of this band, too, with the concomitant reappearance of the band at 1415 cm$^{-1}$. The intensity of the band at 1490 cm$^{-1}$ decreased gradually.

Adsorption of pyridine as a base on the surface of solid acids is one of the most frequently applied methods for the characterization of surface acidity. This adsorption–desorption technique enables the determination of the strength of the interaction between pyridine and the corresponding acid sites present on the surface. The use of IR spectroscopy to detect the adsorbed pyridine enables us to
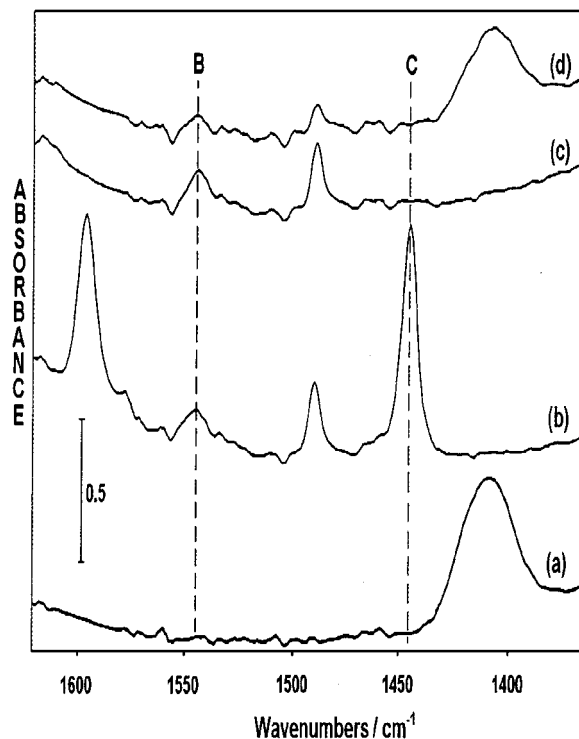


**FIG. 2.** FT-IR spectra illustrating pyridine adsorption on the 13% Nafion-H/silica nanocomposite sample. (B) Band characteristic of pyridine adsorbed on Brønsted sites. (C) Band characteristic of pyridine interacting with the silica matrix. (a) Without pyridine; after pyridine adsorption and evacuation at (b) room temperature, (c) 80°C, and (d) 150°C.

the spectrum of dry Nafion-H and was attributed to $SO_3H$ groups (22). The nanocomposite sample, therefore, has a high concentration of surface $SO_3H$ groups available for catalytic transformation. The 10% Nafion-H/$SiO_2$ specimen has the same weak Lewis acid sites that are thought to be characteristic of the silica surface, but it has a number of fairly strong Brønsted acid sites.

The intensities of the IR bands of the samples cannot be used directly to compare the surface concentration of acid sites of the samples. However, since the matrix (silica) is the same for both materials, the relative intensities of the two bands can be used to make at least a qualitative comparison. The ratios of band intensities corresponding to pyridine bonded to Brønsted and Lewis sites are 1 for 10% Nafion-H/$SiO_2$ and 21.1 for 13% Nafion-H/silica nanocomposite. These normalized data show that the nanocomposite catalyst has a much higher concentration of Brønsted sites.

Cyclopropane is an excellent probe molecule for testing the acidity of solid catalysts (23). It has been shown that ring-opening isomerization of cyclopropane on strongly acidic samples leads to the formation of propene. The product, however, readily undergoes secondary transformations: propene is protonated and subsequently takes part in oligomerization resulting in the formation of oligomers with a carbocationic character on the surface (24–27). As a result of surface oligomerization and protonation, the C=C double bond of propene cannot be detected spectroscopically (28).

The IR spectrum of cyclopropane adsorbed on 10% Nafion-H/$SiO_2$ showed an intense band at 3080 $cm^{-1}$, which is characteristic of cyclopropane species adsorbed on the catalyst surface (23). The intensity of this band decreases with increasing contact time and temperature. The transformation of cyclopropane was found to be slow over this catalyst: the integrated absorbances of the band at 3080 $cm^{-1}$ decreased significantly only at 150°C (Fig. 3).

When the nanocomposite material was treated with cyclopropane, the band related to the adsorbed cyclopropane species (3080 $cm^{-1}$) was detected only at room temperature; the treatment at 80°C induced the transformation of cyclopropane to propene oligomers at a high reaction rate (Fig. 3) (24–27).

The surface reaction of cyclopropane over the two catalyst samples reveals that, once again, the nanocomposite material displays much higher catalytic activity and, consequently, possesses a large number of surface acid centers. The much lower activity of the impregnated sample reflects the considerably lower concentration of the surface-active sites. The silica support was inactive in cyclopropane transformation.

### Catalytic Studies

The results of the catalytic test reactions with the above-mentioned two catalyst samples and comparisons with Nafion-H beads are shown in Tables 1–3.
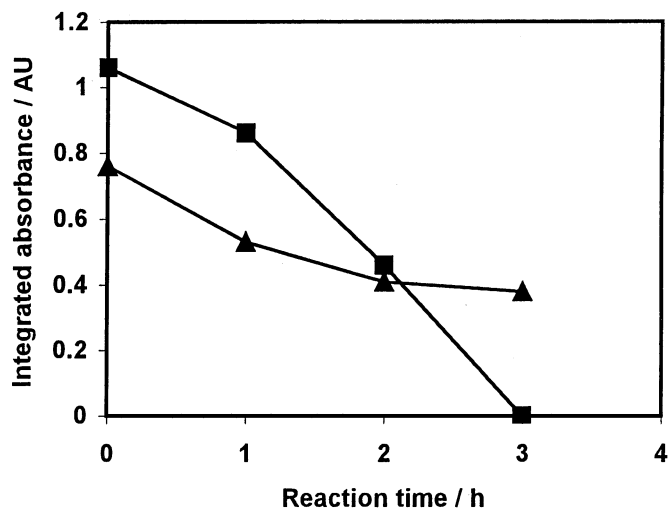


FIG. 3. Consumption of the reactant as a function of contact time in the isomerization of cyclopropane over Nafion-H-based catalysts followed by FT-IR spectroscopy (■, 13% Nafion-H/silica nanocomposite, 80°C; ▲, 10% Nafion-H/$SiO_2$, 150°C).

The adamantylation of toluene with 1-bromoadamantane is a Friedel–Crafts alkylation. The reaction yields two isomeric compounds: p- and m-adamantyltoluene [1] (Table 1). In each case the para isomer, expected on the basis of the orientation effect of the methyl substituent, is

**TABLE 1**

**Conversions and Selectivities of the Adamantylation of Toluene**

| Catalyst samples | Time (min) | Conversion (%) | $r_0^a$ (mmol $min^{-1}$ $gcat^{-1}$) | Selectivity (%) | |
|---|---|---|---|---|---|
| | | | | p | m |
| Nafion-H beads | 5 | 5.4 | $5.02 \times 10^{-2}$ | 85 | 15 |
| | 20 | 16 | | 85 | 15 |
| | 35 | 37.5 | | 82 | 18 |
| | 60 | 51.3 | | 76 | 24 |
| 10% Nafion-H/$SiO_2$ | 5 | 19 | 0.58 | 83 | 17[b] |
| | 20 | 25 | | 85 | 15[c] |
| | 35 | 34 | | 86 | 14 |
| | 60 | 67 | | 82 | 18[d] |
| 13% Nafion-H/silica nanocomposite | 5 | 47 | 3.38 | 80 | 20 |
| | 20 | 100 | | 79 | 21 |
| | 35 | 100 | | 55 | 45 |
| | 60 | 100 | | 61 | 39[b] |

[a] Initial rates.
[b] 4% adamantane.
[c] 2.3% adamantane.
[d] 2% adamantane.
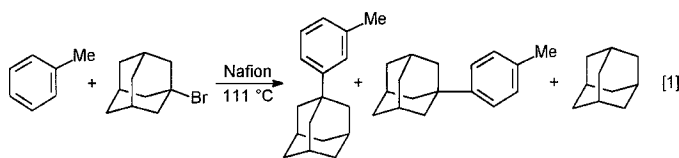
the main product. A large shift in selectivity with time was observed, however, when the nanocomposite was used as the catalyst. This sample exhibited the highest activity of the three catalysts studied. In some cases, small amounts of the adamantane by-product were detected.

It was already shown that, of the three possible isomeric adamantyltoluenes, the ortho isomer is not formed for steric reasons (29). It is also known that acidity exerts a great influence on regioselectivity (29, 30): the distribution of the kinetic product (high excess of the para isomer) can shift to the distribution of the thermodynamic product (increasing ratio of the meta isomer). Since isomerization by alkyl shift is much slower than direct alkylation, this change in product distribution occurs after complete conversion, provided that the catalyst is sufficiently acidic. In the present case, the 13% Nafion/silica nanocomposite sample which, according to IR measurements, had the highest concentration of acid sites, exhibits the highest activity. On the other hand, this catalyst induces a large shift in regioselectivity toward the formation of the meta isomer, approaching a selectivity of 1 : 1, in agreement with results of earlier studies.

The aromatic ortho-Claisen rearrangement has been frequently studied: this transformation results in substituted phenols through the rearrangement of the corresponding allyl ethers (31). Formally, the reaction appears to be a 1,3 O → C migration of the allyl group. In fact, the thermal process is a 3,3 sigmatropic rearrangement and is regarded as being concerted. It is known that acid catalysts, namely, zeolites, are also capable of promoting the Claisen rearrangement (32, 33).

Our results with the Nafion samples show (Table 2) that the rearrangement of allyl phenyl ether (**1**) to o-allyl phenol (**2**), the product of the Claisen rearrangement, is the main direction of the transformation when the silica-supported catalyst is used [2]. The nanocomposite material also shows high selectivity at short reaction time. In

contrast, 2-methyldihydrobenzofuran (**3**), formed as a result of cyclization of **2**, is the main product in the presence of Nafion-H beads. Small amounts of phenol and some oligomerization were also detected. The 10% Nafion/silica and Nafion beads, however, exhibited very low and rapidly declining activity. Again, the nanocomposite sample was more active. However, the rearrangement of the primary product **2**, induced by the highly acidic nature of this catalyst to form the **3** dihydrobenzofuran derivative, results in decreasing selectivity with time. Similar conclusions were reached in a recent study by Sheldon *et al.* who applied H-beta and H-mordenite zeolites (33). Oligomerization, a major side reaction over the latter catalysts, is not very significant in the presence of the nanocomposite sample.

Finally, our catalysts were tested in the Fries rearrangement which is the acid-catalyzed transformation of phenol esters resulting in the formation of phenolic ketones (34). The Lewis acids that were applied originally were later replaced by Brønsted acid catalysts; Nafion-H has been found to be just as active (35, 36).

In the transformation of phenyl acetate (**5**), phenol (**6**) was formed with high selectivity over Nafion beads and in the presence of the silica-supported catalyst [3]; i.e., deacetylation took place (Table 3). This was observed in earlier studies, and the highly reactive ketene thus formed was assumed to bring about deactivation of the catalyst (16, 35). The nanocomposite sample showed some unique characteristics. Firstly, this catalyst again proved to be the most active of the three samples studied (Table 3). Secondly, the Fries rearrangement, leading to 2-hydroxyacetophenone (**7**), 4-hydroxyacetophenone (**8**), and also 4-acetoxyacetophenone (**9**), was more significant over the nanocomposite sample: the combined yield of these three acetylated products (**7**+**8**+**9**) exceeds 50%. Moreover, the transformation becomes completely selective when carried out in the presence of phenol. This

**TABLE 2**

**Conversions and Selectivities of the ortho-Claisen Rearrangement of Allyl Phenyl Ether**

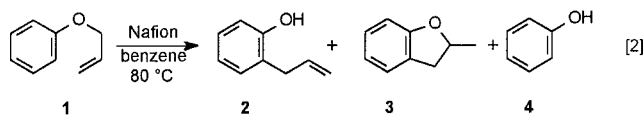| Catalyst samples | Time (h) | Conversion (%) | $r_0$ (mmol min$^{-1}$ gcat$^{-1}$) | Selectivity (%) | | | |
|---|---|---|---|---|---|---|---|
| | | | | **2** | **3** | **4** | oligomers |
| Nafion-H beads | 1 | 1 | 0.25 | 25 | 75 | — | — |
| | 5 | 8 | | 35 | 59 | 6 | — |
| 10% Nafion-H/SiO$_2$ | 1 | 0.5 | 0.025 | 100 | — | — | — |
| | 5 | 9 | | 56.5 | 5.5 | | 33 |
| 13% Nafion-H/silica nanocomposite | 1 | 16 | 1.04 | 50 | 34.5 | 6 | 9 |
| | 5 | 41 | | 27 | 52 | 8 | 13 |

**TABLE 3**

**Conversions and Selectivities of the Fries Rearrangement of Phenyl Acetate**

| Catalyst samples | Time (h) | Conversion (%) | $r_0$ (mmol min$^{-1}$ gcat$^{-1}$) | Selectivity (%) | | | |
|---|---|---|---|---|---|---|---|
| | | | | **6** | **7** | **8** | **9** |
| Nafion-H beads | 1 | 19 | $5.24 \times 10^{-2}$ | 94.5 | — | 5.5 | — |
| | 2 | 24.6 | | 94.5 | — | 5.5 | — |
| 10% Nafion-H/SiO$_2$ | 1 | 2 | $5.52 \times 10^{-3}$ | 100 | — | — | — |
| | 2 | 5 | | 100 | — | — | — |
| 13% Nafion-H/silica nanocomposite | 1 | 45 | 95.4 | 45 | 5 | 24.5 | 25.5 |
| | 2 | 54 | | 46 | 5 | 26 | 23 |
| | 1[a] | 40 | | — | — | 100 | — |

[a] In the presence of phenol.
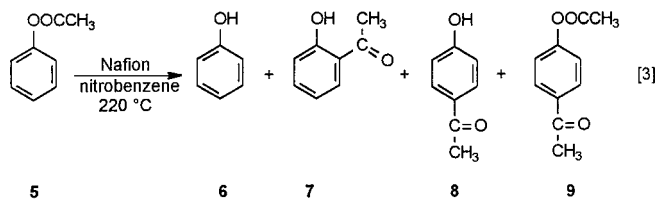


dramatic change was assumed to be brought about by the replenishment of the starting material through the reaction of ketene with phenol (16). A more likely possibility is that phenol acts as a scavenger of the acetyl cation formed in the deacetylation step, thereby directly yielding product **8** through intermolecular acetylation. Such transacetylation has already been demonstrated with zeolite catalysts (37, 38).

Data for a comparison of the activity (initial rates) of the three catalysts in the above transformations are shown in Tables 1–3. It is clear that the 13% Nafion/silica nanocomposite catalyst is the most active of the catalyst samples studied. This is especially true for the Fries rearrangement where the activity of the nanocomposite material is at least 3 orders of magnitude higher than that of the other Nafion samples.

## CONCLUSIONS

Results obtained by using a combination of spectroscopic techniques (pyridine adsorption and ring opening of cyclopropane followed by FT-IR spectroscopy) and catalytic studies show clearly that the 13% Nafion-H/silica nanocomposite sample possesses a large number of surface SO$_3$H groups compared to the silica-supported Nafion-H; this ensures excellent performance in catalytic transformations. This outstanding activity is apparently due to the increased accessibility of surface-active sites to reactants, ensured by the large surface area and the porous structure of the silica matrix.

Data acquired by pyridine adsorption showed that the surface concentration of Brønsted sites of the nanocom-

posite material is about 1 order of magnitude higher than that of the silica-supported sample. The difference in catalytic activity, however, is even more pronounced when the initial rates of the catalytic reactions are compared. This indicates that the concentration of surface-active sites is not the sole factor determining catalytic activity. The excellent activity, i.e., the higher accessibility of protic sites on the surface in the Fries rearrangement, is probably due to the experimental conditions and the favorable steric demand of the reacting molecule.

## ACKNOWLEDGMENTS

## REFERENCES

1. Olah, G. A., and Molnár, Á., "Hydrocarbon Chemistry." Wiley, New York, 1995.
2. Izumi, Y., Urabe, K., and Onaka, M., "Zeolite, Clay and Heteropoly Acid in Organic Reactions." Kodansha, Tokyo/VCH, New York, 1993.
3. Pope, M. T., "Heteropoly and Isopoly Oxometalates." Springer-Verlag, New York, 1983.
4. Ono, Y., and Suzuki, S., in "Acid-Base Catalysis, Proceedings of the International Symposium on Acid-Base Catalysis," p. 379. Sapporo, 1988.
5. Nafion is a registered trademark of E. I. Du Pont de Nemours & Co., Inc.
6. Wieland, S., Auer, E., Freund, A., Lansink Rotgerink, H., and Panster, P., in "Catalysis of Organic Reactions" (R. Malz, Ed.), p. 277. Marcel Dekker, New York, 1996.

7. (a) Olah, G. A., Prakash, G. K. S., and Sommer, J., "Superacids." Wiley Interscience, New York, 1985. (b) Olah, G. A., Iyer, P. S., and Prakash, G. K. S., *Synthesis* 513 (1986).

8. Falk, M., *in* "Perfluorinated Ionomer Membranes" (A. Eisenberg and H. L. Yeager, Eds.), ACS Symposium Series 180, Chap. 8, p. 139. ACS, Wasingthon, DC, 1982.

9. Sondheimer, S. J., Bunce, N. J., and Fyfe, C. A., *J. Macromol. Sci.-Rev. Macromol. Chem. Phys. C* **26**, 353 (1986).

10. Ferry, L. L., *J. Macromol. Sci.-Chem. A* **27**, 1095 (1990).

11. Bascombe, K. N., and Bell, R. P., *J. Chem. Soc.* 1059 (1959).

12. (a) Harmer, M. A., I. P. N. WO95/19222. (b) Harmer, M. A., Farneth, W. E., and Sun, Q., *J. Am. Chem. Soc.* **118**, 7708 (1996).

13. Sun, Q., Harmer, M. A., and Farneth, W. E., *J. Chem. Soc. Chem. Commun.* **1996**, 1201.

14. Sun, Q., Farneth, W. E., and Harmer, M. A., *J. Catal.* **164**, 62 (1996).

15. Sun, Q., Harmer, M. A., and Farneth, W. E., *Ind. Eng. Chem. Res.* **36**, 5541 (1997).

16. Hidekum, A., Harmer, M. A., and Hoelderich, W. F., *J. Catal.* **176**, 260 (1998).

17. Entel, J., Rouf, C. H., and Howard, H. C., *J. Am. Chem. Soc.* **73**, 2365 (1951).

18. Blicke, F. F., and Weinkauff, O. J., *J. Am. Chem. Soc.* **54**, 330 (1932).

19. Basila, M. R., Kantner, T. R., and Rhee, K. H., *J. Phys. Chem.* **68**, 3197 (1964).

20. Parry, E. R., *J. Catal.* **2**, 371 (1963).

21. Karge, H. G., *Z. Phys. Chem., N.F.* **122**, 103 (1980).

22. Ostrowska, J., and Narebska, A., *Colloid Polym. Sci.* **261**, 93 (1983).

23. Kiricsi, I., Hannus, I., Varga, K., and Fejes, P., *J. Catal.* **63**, 501 (1980).

24. Shephard, F. E., Rooney, J. J., and Kemball, C., *J. Catal.* **1**, 379 (1962).

25. Haw, J. F., Richardson, B. R., Osiro, I. S., and Lazo, N. D., *J. Am. Chem. Soc.* **109**, 5278 (1987).

26. Ghosh, A., and Kydd, R. A., *J. Catal.* **100**, 185 (1986).

27. Kofke, G. T. J., and Gorte, R. J., *J. Catal.* **115**, 233 (1989).

28. Kubelkova, L., Novakova, J., Dolejsek, Z., and Jiru, P., *Collect. Czech. Chem. Commun.* **45**, 3101 (1980).

29. Olah, G. A., Török, B., Shamma, T., Török, M., and Prakash, G. K. S., *Catal. Lett.* **42**, 5 (1996).

30. Beregszászi, T., Török, B., Molnár, Á., Olah, G. A., and Prakash, G. K. S., *Catal. Lett.* **48**, 83 (1997).

31. Wipf, P., *in* "Comprehensive Organic Synthesis" (B. M. Trost and I. Fleming, Eds.), Vol. 5: Combining C–C $\pi$-Bonds (L. A. Paquette, Ed.), p. 834. Pergamon Press, Oxford, 1991.

32. Ipaktchi, J., and Brüch, M., *Chem. Ber.* **123**, 1591 (1990).

33. Sheldon, R. A., Elings, J. A., Lee, S. K., Lempers, H. E. B., and Downing, R. S., *J. Mol. Catal. A: Chem.* **134**, 129 (1999).

34. Heaney, H., *in* "Comprehensive Organic Synthesis" (B. M. Trost and I. Fleming, Eds.), Vol. 2: Additions to C–X $\pi$-Bonds, Part 2 (C. H. Heathcock, Ed.), p. 745. Pergamon Press, Oxford, 1991.

35. Olah, G. A., Malhotra, R., Narang, S. C., and Olah, J. A., *Synthesis* 672 (1978).

36. Olah, G. A., Arvanaghi, M., and Krishnamurty, V. V., *J. Org. Chem.* **48**, 3359 (1983).

37. Vogt, A., Kouwenhoven, H. W., and Prins, R., *Appl. Catal. A* **123**, 37 (1995).

38. Jayat, F., Sabater Picot, M. J., and Guisnet, M., *Catal. Lett.* **41**, 181 (1996).